Journal of Cosmology and Astroparticle Physics
An IOP and SISSA journal

Received: October 23, 2024
Accepted: January 24, 2025
Published: March 26, 2025

Polar magnetic fields in black-hole space-times

R. Kerner,[a] **G. Koekoek**,[b,c] **J.A. Schuring**[b,c] **and J.W. van Holten**[c,d]

[a] *Laboratoire de Physique Théoretique de la Matière Condensée, Sorbonne University, Paris, France*
[b] *Department of Gravitational Waves and Fundamental Physics, Maastricht University, Duboidsomein 30, Maastricht, The Netherlands*
[c] *Nikhef, Science Park 105, Amsterdam, The Netherlands*
[d] *Lorentz Institute, Leiden University, Niels Borhweg 2, Leiden, The Netherlands*

E-mail: richard.kerner@upmc.fr, gideon.koekoek@maastrichtuniversity.nl, julia@pnpmedia.nl, t32@nikhef.nl

Abstract: We study the motion of charged test particles in the combined gravitational and axially symmetric electromagnetic fields of a static Schwarzschild and slowly rotating Kerr spacetimes, in particular considering the conditions for circular equatorial orbits. We present a series calculation of the electromagnetic fields under the boundary condition that they are to vanish at infinity, and verify these with the closed-form expressions obtained previously in literature. Such particle orbits always exist in odd-multipole magnetic fields, and they can exist for particular radii in a combination of two or more even-multipole magnetic fields. Combinations of several odd-multipole fields can give rise to radial variation in the field orientation and the direction of motion of charged particles. Deviations from circularity are described using a perturbative approach. This also allows to study the stability of the parent circular orbits.

Keywords: astrophysical black holes, Exact solutions, black holes and black hole thermodynamics in GR and beyond, GR black holes, magnetic fields

ArXiv ePrint: 2407.04975

© 2025 The Author(s). Published by IOP Publishing Ltd on behalf of Sissa Medialab. Original content from this work may be used under the terms of the Creative Commons Attribution 4.0 licence. Any further distribution of this work must maintain attribution to the author(s) and the title of the work, journal citation and DOI.

https://doi.org/10.1088/1475-7516/2025/03/065

JCAP03(2025)065

Contents

JCAP03(2025)065

1 Introduction

Compact astrophysical objects are frequently accompanied by extended magnetic fields. These fields can have their origin in the object itself, as happens with white dwarfs or neutron stars, or they are caused by external currents of charged matter like accretion disks, as is particularly relevant for black holes [1, 2].

Configurations of magnetic fields in the background of Schwarzschild or Kerr geometries have been studied by many authors [3]–[10]; such an approximate description of the solutions of the Einstein-Maxwell equations are relevant when the back reaction of the external electromagnetic field on the space-time geometry can be neglected, i.e. when the effect of the energy density in this field on the space-time curvature is sufficiently small, as is often the case. These weak fields are sometimes refered to as test fields.

In this paper we review some of the earlier results and then proceed to study the motion of charged particles in the combined gravitational and electromagnetic background, first of

all in a Schwarzschild background. Charged particle motion, in particular on circular orbits, has been widely studied [11]–[17]. Here we extend the analysis by considering in detail the conditions for their stability, and by allowing non-circular orbits as well. In addition we show that combinations of different multipole fields allow discrete orbits that would not exist in only a dipole or single higher-order multipole field by itself.

After considering magnetic fields in the static Schwarzschild geometry we also address weakly rotating compact objects in the context of the linear approximation of a Kerr background. In that case in the frame of a static observer at asymptotically large distance any static axisymmetric magnetic field is necessarily accompanied by radial and polar electric fields. We conclude by summarizing our results; many details of our calculations are collected in the appendices. Throughout this paper results are expressed in natural units in which the speed of light $c = 1$.

2 Static magnetic fields in Schwarzschild space-time

Full analytic expressions for static and axially symmetric magnetic test fields in Schwarzschild space-time have been derived by several authors. The precise form depends on the boundary conditions. A particular solution which has been much studied is expressed in terms of the Killing vectors of the underlying static and spherically symmetric space [3]; magnetic test fields of this type are asymptotically uniform and finite.

In the present paper we consider test fields which are localized around stars and black holes and vanish at asymptotically large distances; their structure close to the surface or horizon can still be allowed to vary, depending on the source of the magnetic field. In the case of a static and spherically symmetric space-time, employing standard Schwarzschild-Droste co-ordinates (reviewed in appendix A), one can fix a gauge such that the electro-magnetic vector potential has only one non-vanishing component A_φ, satisfying the equation [4]–[12]

$$r^2\partial_r\left[\left(1-\frac{2GM}{r}\right)\partial_r A_\varphi\right]+\sin\theta\partial_\theta\left[\frac{1}{\sin\theta}\partial_\theta A_\varphi\right]=-r^4\sin^2\theta\, j^\varphi, \tag{2.1}$$

where j^φ is the density of a current circulating the black hole and acting as a source for the magnetic field. Details of the derivation are given in appendix B.

In regions where the current density vanishes: $j^\varphi = 0$, the equation becomes separable; taking a potential defined by a product

$$A_\varphi = f(r)\Phi(\cos\theta), \tag{2.2}$$

the factors are related by coupled ordinary differential equations in r and $x = \cos\theta$:

$$r^2\frac{d}{dr}\left[\left(1-\frac{2GM}{r}\right)\frac{df}{dr}\right]=\lambda f, \quad \text{and} \quad (1-x^2)\frac{d^2\Phi}{dx^2}=-\lambda\Phi, \tag{2.3}$$

where λ is a constant common eigenvalue of the operators acting on $\Phi(x)$ and $f(r)$. For the angular component $\Phi(x)$ there exists a complete set of eigenfunctions $\Phi_l(x)$ defined in terms of the Legendre polynomials $P_l(x)$, $l = 0, 1, 2, \ldots$, by

$$\Phi_l(x) = (1-x^2)\frac{dP_l}{dx} = l\left(P_{l-1}(x) - xP_l(x)\right). \tag{2.4}$$

JCAP03(2025)065

For $l = 0$ this implies that $\Phi_0(x) = 0$, therefore in the spectrum of Φ_l the value $l = 0$ may be disregarded. Note that, as the Legendre polynomials are solutions of the equations

$$\frac{d}{dx}\left[\left(1-x^2\right)\frac{dP_l}{dx}\right] = -l(l+1)\,P_l(x), \tag{2.5}$$

it follows that

$$\frac{d\Phi_l}{dx} = -l(l+1)P_l(x). \tag{2.6}$$

Combining the above definitions and relations one then gets

$$(1-x^2)\,\frac{d^2\Phi_l}{dx^2} = -l(l+1)\Phi_l(x). \tag{2.7}$$

Thus we obtain a complete set of solutions for the second equation (2.3) with eigenvalues

$$\lambda = l(l+1), \qquad l = 1, 2, \ldots \tag{2.8}$$

It then remains to solve for the corresponding radial functions $f_l(r)$ to obtain the general form of the vector potential in the form of a series:

$$A_\varphi(r,\theta) = \sum_{l=l}^{\infty} f_l(r)\Phi_l(\cos\theta). \tag{2.9}$$

The radial functions satisfy the eigenvalue equation (2.3) with the eigenvalues (2.8). This equation has two kinds of solutions [4]; first there are solutions expressed in terms of an infinite series in powers of $1/r$:

$$f_l(r) = \sum_{n=l}^{\infty} c_n^{(l)} \left(\frac{2GM}{r}\right)^n, \tag{2.10}$$

with the coefficients related to the first one by

$$c_{l+k}^{(l)} = \frac{1}{k!}\prod_{m=1}^{k}\left(\frac{(l+m)^2-1}{2l+m+1}\right) c_l^{(l)}, \qquad k = 1, 2, \ldots \tag{2.11}$$

These solutions are therefore defined by a single free normalization parameter $c_l^{(l)}$. As by construction they vanish in the limit $r \to \infty$, they are relevant especially — but not exclusively — in the large-r region.

In addition to the infinite series solutions vanishing at infinity there exist polynomial solutions

$$A_\varphi(r,\theta) = \sum_{l=l}^{\infty} g_l(r)\Phi_l(\cos\theta), \tag{2.12}$$

with

$$g_l(r) = \sum_{n=2}^{l+1} a_n^{(l)} \left(\frac{r}{2GM}\right)^n. \tag{2.13}$$

JCAP03(2025)065

Here $a_2^{(l)}$ is a free parameter, in terms of which the other coefficients are given by

$$a_{2+k}^{(l)} = \prod_{m=1}^{k} \left(\frac{m(m+1) - l(l+1)}{m(m+2)} \right) a_2^{(l)}, \quad k = 1, \ldots, l-1. \tag{2.14}$$

Obviously these solutions do not vanish asymptotically for large r; therefore they can be relevant at most in a finite domain of r-values in the inner region of the magnetic field. It should be noted that the radial functions $f_l(r)$ presented in series form above can be written in closed form [4, 8]

$$f_l(r) = r^2 \mathcal{Q}_{l-1}^{(0,2)} \left(\frac{r}{MG} - 1 \right), \tag{2.15}$$

in which $\mathcal{Q}_{l-1}^{(0,2)}$ is the Jacobi function of the second kind. The polynomial solutions $g_l(r)$ are related to the Jacobi polynomial $\mathcal{P}_{l-1}^{(0,2)}$ of the second kind by

$$g_l(r) = r^2 \, \mathcal{P}_{l-1}^{(0,2)} \left(\frac{r}{MG} - 1 \right). \tag{2.16}$$

More details are given in appendix D. Also the angular functions $\Phi_l(x)$ are related to Gegenbauer polynomials by [4]

$$\Phi_l(x) = (1 - x^2) C^{3/2}(x). \tag{2.17}$$

In the following we focus on the series solutions which vanish at infinity. From the vector potentials (2.9) one derives two non-vanishing components of the Maxwell tensor:

$$F_{r\varphi} = \sum_{l=1}^{\infty} f_l'(r) \Phi_l(\cos\theta), \qquad F_{\theta\varphi} = \sin\theta \sum_{l=1}^{\infty} l(l+1) \, f_l(r) P_l(\cos\theta). \tag{2.18}$$

The corresponding components of the magnetic field strength $B_i = \tilde{F}_{0i}$, as defined in appendix B, are

$$B_r = \frac{1}{r^2} \sum_{l=1}^{\infty} l(l+1) \, f_l(r) P_l(\cos\theta), \quad B_\theta = -\frac{1}{\sin\theta} \left(1 - \frac{2GM}{r} \right) \sum_{l=1}^{\infty} f_l'(r) \Phi_l(\cos\theta), \tag{2.19}$$

whilst the azimuthal component vanishes: $B_\varphi = 0$.

Dipole fields. The lowest and often dominant component of the magnetic field is of dipole form with $l = 1$; in that case

$$P_1(\cos\theta) = \cos\theta, \qquad \Phi_1(\cos\theta) = 1 - \cos^2\theta, \tag{2.20}$$

and

$$\begin{aligned} f_1(r) &= c_1^{(1)} \frac{2GM}{r} \left(1 + \frac{3}{2} \frac{GM}{r} + \frac{12}{5} \left(\frac{GM}{r} \right)^2 + \ldots \right), \\ f_1'(r) &= -c_1^{(1)} \frac{2GM}{r^2} \left(1 + 3 \, \frac{GM}{r} + \frac{36}{5} \left(\frac{GM}{r} \right)^2 + \ldots \right). \end{aligned} \tag{2.21}$$

JCAP03(2025)065

These expressions can actually be written in closed form as

$$f_1(r) = -\frac{3c_1^{(1)}}{2}\left(\frac{r^2}{2G^2M^2}\ln\left(1-\frac{2GM}{r}\right)+\frac{r}{GM}+1\right),$$
$$f_1'(r) = -\frac{3c_1^{(1)}}{2GM}\left(\frac{r}{GM}\ln\left(1-\frac{2GM}{r}\right)+\frac{1}{1-\frac{2GM}{r}}+1\right). \tag{2.22}$$

The non-vanishing magnetic field components then have expansions

$$B_r = \frac{2\mu}{r^3}\cos\theta\left(1+\frac{3GM}{2r}+\dots\right), \qquad B_\theta = \frac{\mu}{r^2}\sin\theta\left(1+\frac{GM}{r}+\dots\right), \tag{2.23}$$

with the magnetic dipole moment μ defined by

$$\mu = 2GMc_1^{(1)}. \tag{2.24}$$

Note that the corresponding polynomial solution with $l = 1$ follows from

$$g_1(r) = a_2^{(1)}\left(\frac{r}{2GM}\right)^2, \quad g_1'(r) = a_2^{(1)}\frac{r}{2(GM)^2}, \tag{2.25}$$

and gives rise to magnetic fields

$$B_r = B_z\cos\theta, \qquad B_\theta = -B_z\,(r-2GM)\sin\theta, \tag{2.26}$$

where B_z is the constant magnetic field strength on the positive z-axis:

$$B_z = \frac{a_2^{(1)}}{2(GM)^2}. \tag{2.27}$$

This magnetic field is purely transverse in the equatorial plane and purely radial along the z-axis. This is the asymptotically constant field found in ref. [3] specialized to the Schwarzschild case. In view of the boundary conditions at infinity we will not consider this solution in the following.

3 The motion of charged test particles

The motion of massive test particles in combined gravitational and magnetic fields is decribed by a world line $\xi^\mu(\tau)$ with tangent vector $u^\mu = \dot{\xi}^\mu$, which are solutions of the covariant Lorentz force equation

$$\dot{u}^\mu + \Gamma_{\lambda\nu}{}^{\mu}(\xi)u^\lambda u^\nu = \frac{q}{m}F^\mu{}_\nu(\xi)u^\nu. \tag{3.1}$$

Here the overdot denotes a proper-time derivative: $\dot{\xi} = d\xi/d\tau$; the forces are local, being dictated by the values of the Riemann-Christoffel connection and the Maxwell tensor at the location of the world line. Our conventions for the metric and components of the connection in a Schwarzschild space-time are given in appendix A. The Maxwell tensor $F_{\mu\nu}$ has non-zero components $F_{r\varphi}$ and $F_{\theta\varphi}$ given in equation (2.18).

JCAP03(2025)065

As both the background geometry and the magnetic field are static, and they share axial symmetry, the energy and the angular momentum component in the z-direction of test particles are conserved. Indeed it is straightforward to check, using polar co-ordinates $\xi^\mu = (t, r, \theta, \varphi)$, that the following are constants of motion:

$$\varepsilon = \left(1 - \frac{2GM}{r}\right) u^t, \qquad \ell = r^2 \sin^2\theta \, u^\varphi + \frac{q}{m} A_\varphi. \tag{3.2}$$

In addition, by definition of the proper time there is a constraint

$$g_{\mu\nu}(\xi) u^\mu u^\nu = -1. \tag{3.3}$$

Eliminating u^t and u^φ in terms of the constants of motion (3.2) this becomes

$$u^{r\,2} + \left(1 - \frac{2GM}{r}\right) r^2 u^{\theta\,2} = \varepsilon^2 - \left(1 - \frac{2GM}{r}\right)\left[1 + \frac{1}{r^2 \sin^2\theta}\left(\ell - \frac{q}{m} A_\varphi\right)^2\right]. \tag{3.4}$$

The θ-component of the world line equation (3.1) can be written as

$$\frac{d}{d\tau}\left(r^2 u^\theta\right) = \sin\theta \cos\theta \, r^2 u^{\varphi\,2} + \frac{q}{m} F_{\theta\varphi} \, u^\varphi. \tag{3.5}$$

Now recall, that for even $l = 2n$ the polynomials $P_l(\cos\theta)$ and $\Phi_l(\cos\theta)$ in the equatorial plane take the values

$$P_{2n}(0) = \frac{(-1)^n}{2^{2n}} \frac{(2n)!}{(n!)^2} \quad \text{and} \qquad \Phi_{2n}(0) = 0, \tag{3.6}$$

whilst for odd $l = 2n + 1$

$$P_{2n+1}(0) = 0, \qquad \Phi_{2n+1}(0) = (2n+1) P_{2n}(0) = \frac{(-1)^n}{2^{2n}} \frac{(2n+1)!}{(n!)^2}. \tag{3.7}$$

It follows that the individual contributions of the even-l multipole fields to the magnetic field strength $F_{\theta\varphi}$ in the equatorial plane never vanish, and charged particles in non-radial orbits experience a transverse Lorentz force. Indeed in the equatorial plane $\cos\theta = 0$, in a magnetic multipole field with $l = 2n$

$$\frac{d}{d\tau}\left(r^2 u^\theta\right)_{l=2n} = \frac{q\ell}{mr^2} \, 2n(2n+1) f_{2n}(r) P_{2n}(0).$$

This vanishes only on radial trajectories, with $\ell = 0$. In contrast, for odd multipoles with $l = 2n + 1$ the magnetic field in the equatorial plane is perpendicular to that plane, and the Lorentz-force component on the right-hand side of equation (3.5) vanishes there. Planar equatorial orbits then exist in odd multipole fields with

$$r^2 u^\varphi = \ell - \frac{q}{m} (2n+1) P_{2n}(0) \, f_{2n+1}(r). \tag{3.8}$$

Note however, that although individual even-l multipole fields do not allow for planar equatorial orbits, whenever there are several of these multipole fields they will in general cancel each other in the equatorial plane for specific values of the radial co-ordinate r,

JCAP03(2025)065

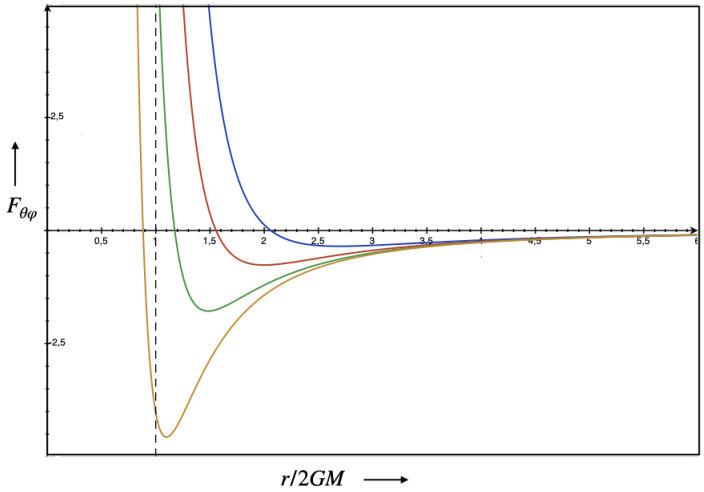

Figure 1. $F_{\theta\varphi}$ as a function of $r/2GM$ in the equatorial plane for combinations of quadrupole and hexadecapole fields with relative strength 1 (blue), 1/2 (red), 1/4 (green) and 1/8 (yellow); the last one has no zero-point outside the horizon.

depending on the relative strengths as determined by the coefficients $c_l^{(l)}$; this is clear from the alternating signs in (3.6). As a consequence there exist circular orbits at characteristic radius $r = R$ such that

$$\sum_{n=1}^{\infty} 2n(2n+1)P_{2n}(0)f_{2n}(R) = 0. \tag{3.9}$$

As an example $F_{\theta\varphi}$ is plotted in figure 1 as a function of $r/2GM$ for several combinations of quadrupole ($l = 2$) and hexadecapole ($l = 4$) fields.

Where $F_{\theta\varphi} = 0$ a stable circular orbit exists, provided it lies outside the horizon $r/2GM = 1$ and the satisfies stability conditions to be discussed later on.

Figure 2 shows $F_{r\varphi}$ for similar combinations of dipole ($l = 1$) and octopole ($l = 3$) fields. The absolute values depend on the scale set by $c_1^{(1,2)}$; however the zeros are not affected by the scale. These combinations of odd multipole fields allow for equatorial orbits of any radius outside the horizon meeting all stability criteria, but whenever $F_{r\varphi} = 0$ the magnetic field and the Lorentz force on charges moving in the equatorial plane changes sign.

4 Circular equatorial orbits

Generic circular orbits in the equatorial plane with fixed $r = R$ exist for dipole and other odd-l multipole fields. On circular orbits both the radial velocity and the radial acceleration vanishes. They also require $F_{\theta\varphi}(R, \pi/2) = 0$. Writing $u^\varphi = \omega_R$ the radial component of equation (3.1) then implies

$$\left(1 - \frac{2GM}{R}\right)\left(\frac{GM}{R^3}\,u^{t\,2} - \omega_R^2\right) = -\frac{qB_\theta}{mR}\,\omega_R, \tag{4.1}$$

with B_θ as defined in (2.19). In addition the constraint (3.3) with $u^r = u^\theta = 0$ becomes:

$$\left(1 - \frac{2GM}{R}\right)u^{t\,2} = 1 + R^2\omega_R^2. \tag{4.2}$$

JCAP03(2025)065

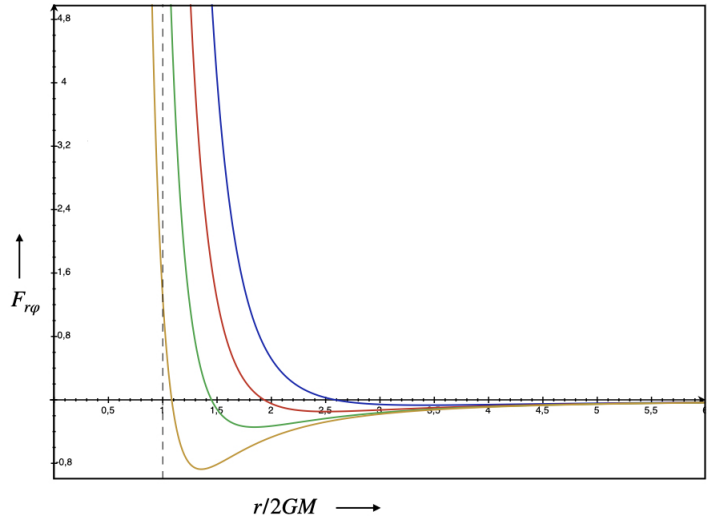

Figure 2. $F_{r\varphi}$ as a function of $r/2GM$ in the equatorial plane for combinations of dipole and octopole fields with relative strength 1 (blue), 1/2 (red), 1/4 (green) and 1/8 (yellow).

Combining these results provides a relation between the angular velocity and the orbital radius:

$$\left(1-\frac{3GM}{R}\right)\omega_R^2-\frac{qB_\theta}{mR}\,\omega_R=\frac{GM}{R^3}. \tag{4.3}$$

For all values of $R\neq 3GM$ this quadratic equation for ω_R has general solutions

$$R\omega_R=\frac{1}{1-\frac{3GM}{R}}\left(\frac{qB_\theta}{2m}\pm\sqrt{\frac{GM}{R}\left(1-\frac{3GM}{R}\right)+\left(\frac{qB_\theta}{2m}\right)^2}\right). \tag{4.4}$$

However, provided $qB_\theta\neq 0$, for the special circular orbit at $R=3GM$ the equation reduces to a linear one, in which case

$$R\omega_R=-\frac{m}{3\,qB_\theta},\qquad R=3GM. \tag{4.5}$$

For electrically neutral particles, or in the absence of a magnetic field, this circular orbit is available only to massless particles like photons. A number of physically relevant solutions (4.4) have been plotted in figure 3 for $R>2GM$.

Solutions for test particles with opposite charge or opposite magnetic field strength, such that $qB_\theta\to -qB_\theta$, are related by opposite angular velocity: $\omega_R\to-\omega_R$. For each of these cases there is always a solution with $R>3GM$. From eq. (4.4), it follows that a second solution with $2GM<R<3GM$ also exists provided

$$\left(\frac{qB_\theta}{m}\right)^2\geq\left(\frac{2GM}{R}\right)^2\left(3-\frac{R}{GM}\right). \tag{4.6}$$

When this condition is not met, no circular orbit inside $3GM$ exists.

Two extreme cases are $q=0$ when only gravity acts:

$$\omega_R^{\pm}=\pm\sqrt{\frac{GM}{R^3}\frac{1}{1-\frac{3GM}{R}}}; \tag{4.7}$$

JCAP03(2025)065

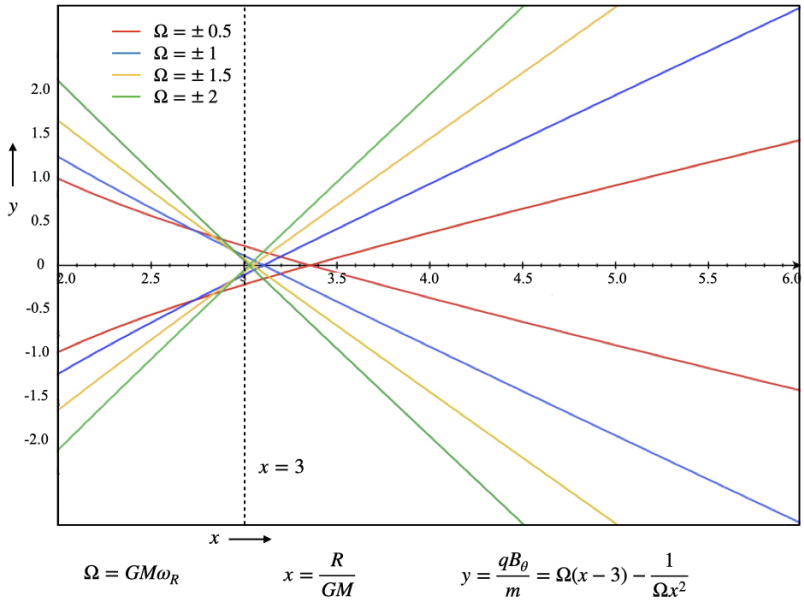

Figure 3. Solutions of equation (4.4).

and $GM = 0$ when there is only a magnetic field causing cyclotron motion:

$$\omega_R^- = 0, \qquad \omega_R^+ = \frac{qB_\theta}{mR}. \tag{4.8}$$

5 More on bound equatorial orbits

Starting from the circular orbits discussed in the previous section, one can construct more general bound motions using the method of relativistic epicycles [19, 20]. In this procedure bound orbits are obtained as deformations of circular motion in a perturbative expansion. In this paper we discuss only first-order deviations from circular motion; these deviations also provide information on the stability of circular orbits. It is straightforward to extend the procedure to higher orders [21, 22].

The deviation of any bound orbit from a circular one is parametrized by $\xi^\mu = \xi_0^\mu + n^\mu$, where to first order the deviation n^μ is a solution of the extended relativistic deviation equation

$$\frac{D^2 n^\mu}{D\tau^2} = R_{\kappa\nu\lambda}{}^{\mu}\, u^\kappa u^\lambda n^\nu + \frac{q}{m}\, T^\mu, \tag{5.1}$$

where

$$T^\mu = F^\mu_{\ \nu} \frac{Dn^\nu}{D\tau} + n^\nu D_\nu F^\mu_{\ \lambda} u^\lambda. \tag{5.2}$$

In these expressions the Riemann curvature $R_{\kappa\nu\lambda}{}^{\mu}(\xi_0)$, the magnetic field strength $F^\mu_{\ \nu}(\xi_0)$ and the proper velocity $u^\mu = \dot{\xi}_0^\mu$ are evaluated on the circular reference orbit [18].

We first consider deviations out of the equatorial plane, parametrized by n^θ. As on a circular equatorial orbit $u^r = u^\theta = \cos\theta = 0$ and we require $F_{\theta\varphi} = 0$ in the plane, it follows

JCAP03(2025)065

that the various contribution combine to

$$\begin{aligned}\ddot{n}^\theta &= -\frac{GM}{R^3}\left[\left(1-\frac{2GM}{R}\right)u^{t\,2}+2R^2u^{\varphi\,2}\right]n^\theta+\frac{qu^\varphi}{mR^2}\left[R\left(1-\frac{2GM}{R}\right)F_{r\varphi}+\partial_\theta F_{\theta\varphi}\right]n^\theta\\ &= -\left(\omega_R^2+\frac{q\nu_R}{m}\,\omega_R\right)n^\theta, \quad \text{where} \quad \nu_R=\left.\frac{dB_r(R)}{d\cos\theta}\right|_{\cos\theta=0}.\end{aligned} \tag{5.3}$$

Clearly the orbital deviations in the plane do not mix with the resulting periodic transverse motion, and hence can be treated separately. The solutions of eq. (5.3) are periodic with frequency ω_θ given by

$$\omega_\theta^2=\omega_R^2\left(1+\frac{q\nu_R}{m\omega_R}\right), \tag{5.4}$$

unless the squared frequency ω_θ^2 becomes negative, for $q\nu_R/m\omega_R<-1$. This value represents the limit of stabilty of the orbit with respect to transverse fluctuations.

The remaining components of the deviation vector n^μ are coupled by eq. (5.2) and can be expressed in the form

$$\begin{pmatrix} \frac{d^2}{d\tau^2} & \alpha\frac{d}{d\tau} & 0\\ \beta\frac{d}{d\tau} & \frac{d^2}{d\tau^2}-\kappa & -\gamma\frac{d}{d\tau}\\ 0 & \eta\frac{d}{d\tau} & \frac{d^2}{d\tau^2}\end{pmatrix}\begin{pmatrix} n^t\\ n^r\\ n^\varphi\end{pmatrix}=0, \tag{5.5}$$

where

$$\begin{aligned}\alpha &= \frac{2GM}{R^2}\frac{u^t}{1-\frac{2GM}{R}}, & \beta &= \frac{2GM}{R^2}\left(1-\frac{2GM}{R}\right)u^t,\\ \gamma &= \left(1-\frac{2GM}{R}\right)2Ru^\varphi-\frac{qB_\theta}{m}, & \eta &= \frac{2u^\varphi}{R}-\frac{qB_\theta}{mR^2}\frac{1}{1-\frac{2GM}{R}},\\ \kappa &= 3\left(1-\frac{2GM}{R}\right)u^{\varphi\,2}-\frac{2qB_\theta u^\varphi}{mR}\frac{R-3GM}{R-2GM}-\frac{qB'_\theta\,u^\varphi}{m}\\ &= \frac{3GM}{R^3}\frac{R-2GM}{R-3GM}+\frac{qB_\theta\,\omega_R}{mR}\frac{R^2-6G^2M^2}{(R-2GM)(R-3GM)}-\frac{qB'_\theta\,\omega_R}{m}.\end{aligned} \tag{5.6}$$

Here $B'_\theta(R)=(\partial_r B_\theta)(R)$. The eigenvalues $i\tilde{\omega}$ of the operator $d/d\tau$ in equation (5.5) are solutions of the characteristic equation

$$\tilde{\omega}^4\left(\tilde{\omega}^2-\eta\gamma+\alpha\beta+\kappa\right)=0. \tag{5.7}$$

Apart from the zero-modes, the solutions are

$$\begin{aligned}\tilde{\omega}^2 = &\frac{GM}{R^3}\frac{R-6GM}{R-3GM}-\frac{qB_\theta\,\omega_R}{mR}\frac{R^2-4GMR+6G^2M^2}{(R-2GM)(R-3GM)}\\ &+\left(\frac{qB_\theta}{m}\right)^2\frac{1}{R(R-2GM)}+\frac{qB'_\theta\,\omega_R}{m},\end{aligned} \tag{5.8}$$

resulting in periodic expressions for n^t, n^r, n^φ for real frequencies $\tilde{\omega}$.

As in general the period of the deviations is different from that of the circular orbit, the periastron will perform a precession the phase of which is determined by the ratio of

JCAP03(2025)065

the angular frequencies; more precisely, with $n^r(\tau) = n^r(0)\cos\tilde{\omega}\tau$ it follows that the angles of two periastra at proper time $\tau = 0$ and τ_n differ by

$$\tilde{\omega}\tau_n = n\pi \quad \Rightarrow \quad \varphi(\tau_n) - \varphi(0) = \frac{\omega_R}{\tilde{\omega}}\, n\pi. \tag{5.9}$$

Following the criterion for transverse stability, orbital stability for fluctuations in the equatorial plane requires the squared frequency eq. (5.8) to be non-negative, whereas exponentially run-away solutions are found when it is negative. Thus unstable orbits are possible for appropriate strength and sign of the magnetic interaction term qB_θ.

Specifying to a single-multipole magnetic field of rank l, eq. (2.19) implies

$$B'_{l\theta} = \left(\frac{2GM}{R^2} \frac{1}{1 - \frac{2GM}{R}} + \frac{f''_l}{f'_l} \right) B_{l\theta} \tag{5.10}$$

the orbital frequency ω_R is expressed in terms of the magnetic field $B_{l\theta}$, and the limit of planar stability $\tilde{\omega}^2 = 0$ becomes a quadratic equation for $B_{l\theta}$, which can easily be solved algebraically.

6 Kinematical stability of circular orbits for dipole fields

We will now collect results on the existence and stability of circular orbits in a Schwarzschild space-time, applying them to the special case of a dipole field with $l = 1$. We use the dimensionless quantities introduced in figure 3;

$$x = \frac{R}{GM}, \qquad \Omega = GM\omega_R, \qquad y = \frac{qB_\theta}{m}. \tag{6.1}$$

As we consider the exterior of horizon, $x > 2$. By eq. (2.23)

$$y = \frac{q\mu}{m(GMx)^2}\, h(x), \tag{6.2}$$

where using eq. (2.22)

$$h(x) = \frac{3}{4}\left(1 - \frac{2}{x}\right) x^2 \left(1 + \frac{1}{1 - \frac{2}{x}} + x \ln\left(1 - \frac{2}{x}\right) \right). \tag{6.3}$$

But eq. (4.3) states that the dimensionless magnetic field expressed in terms of x and Ω is

$$y(x, \Omega) = (x - 3)\,\Omega - \frac{1}{x^2\Omega}. \tag{6.4}$$

Combining these results we find for $\Omega(x)$ in terms of the physical data (q, μ, m, M) the expression

$$\frac{\Omega}{y} = \frac{1}{2(x-3)} \left(1 \pm \sqrt{1 + \frac{4(x-3)}{x^2 y^2}} \right). \tag{6.5}$$

Real solutions for Ω exist iff.

$$y^2 + \frac{4}{x^2}\,(x - 3) \geq 0. \tag{6.6}$$

This inequality is automatically satisfied for all y if $x > 3$. The circular motion is stable against fluctuations in the transverse direction (out of the plane) provided $\omega_\theta^2 > 0$; in view of eq. (5.4) this requires

$$\frac{q\nu_R}{m\omega_R} > -1.$$

JCAP03(2025)065

Now for $l = 1$, using eq. (2.3)

$$\nu_R|_{l=1} = \frac{2\mu}{(GMx)^3}\,k(x), \qquad k(x) = -\frac{3}{4}x\left(\frac{x^2}{2}\ln\left(1-\frac{2}{x}\right)+x+1\right). \tag{6.7}$$

Therefore stability requires

$$\frac{y}{\Omega} > -\frac{xh(x)}{2k(x)}. \tag{6.8}$$

This is always satisfied if $y/\Omega > 0$. Combining this inequality with (6.4) it follows that

$$\Omega^2 > \frac{2k(x)}{x^2\left[2(x-3)k(x)+xh(x)\right]}. \tag{6.9}$$

We can also eliminate Ω to get another inequality for y:

$$\frac{4(x-3)k(x)}{xh(x)}\,\frac{1}{1\pm\sqrt{1+\frac{4(x-3)}{x^2y^2}}} > -1, \quad \frac{k(x)}{h(x)} = 1+\frac{1}{2x}+\frac{7}{10x^2}+\frac{11}{10x^3}+\ldots \tag{6.10}$$

This inequality holds automatically if the l.h.s. is positive, which happens with the plus sign for the square root for all y and $x > 3$. Finally the circular motion must be stable under fluctuations in the equatorial plane, which imposes the condition $\tilde{\omega}^2 > 0$. Now for a dipole field

$$\frac{qB'_\theta}{m} = \frac{1}{GM}\frac{dy}{dx} = -\frac{2q\mu}{m(GMx)^3}\,k(x) = -\frac{2k(x)}{R\,h(x)}\,y \tag{6.11}$$

and hence stability under fluctuations in the equatorial plane follows via eq. (5.8) as

$$1+\frac{(x-2)(x-6)}{x^2(x-3)y^2}-\frac{\Omega}{y}\left(\frac{x^2-4x+6}{x-3}+2(x-2)\frac{k(x)}{h(x)}\right) \geq 0. \tag{6.12}$$

The results in equations (6.6), (6.10) and (6.12) provide implicit formulae for the curves dividing allowed stable regions from unstable regions in the (x, y)-plane. The results are shown in figure 4, where the magnetic field strength is quantified in terms of the dipole moment μ. The key features are the regions separated by the colored lines. The red line denotes the dividing line between kinematically allowed and disallowed orbits, where all of the region above the red line is allowed. The solid (dashed) blue line denotes the dividing line between planar stability and instability for orbits with minus (plus) sign in eq. (6.5), where the region above (below) the blue line is stable. The solid (dashed) green line denotes the dividing line between transverse stability and instability for orbits with minus (plus) sign in eq. (6.5), where for both signs the region right of the corresponding green line is stable. Analytical details are provided in appendix E. An important feature is that, in case of the minus sign, the smallest radius of equatorially stable circular orbits shifts from $R/GM = 6$ to 3, while simultaneously the smallest radius of kinematically allowed circular orbit shifts from $R/GM = 3$ to the horizon of the black hole at $R/GM = 2$. This is the result of gravitational attraction being counterbalanced by the Lorentz-force.

Note that in this section we have only considered the kinematical stability of circular orbits. In a complete treatment one would also have to consider the emission of electromagnetic and gravitational radiation, which ultimately destabilizes any classical bound orbit.

JCAP03(2025)065

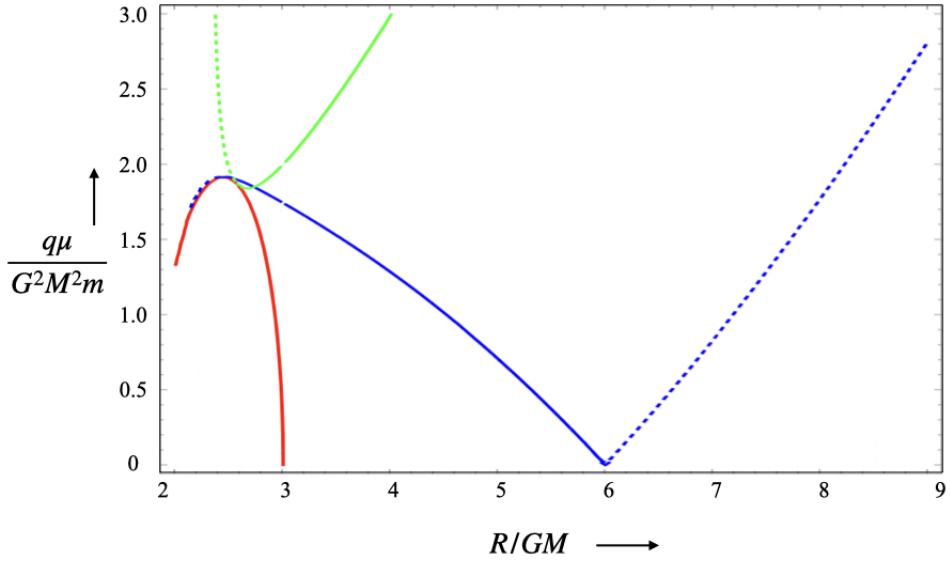

Figure 4. Regions of existence, and planar and perpendicular stabilities, for the orbits with plus and minus sign in eq. (6.5). The red line denotes the dividing line between kinematically allowed and disallowed orbits, the blue lines separates equatorial stability from instability, and the green lines separates transverse stability from instability. The resulting regions are described in the main text.

7 Magnetic fields of slowly rotating stars

In the limit of slow rotation and distances $r \gg 2GM$ (that is, to first order in G) the line element of Kerr space-time takes the form of the Lense-Thirring metric

$$ds^2 \simeq -\left(1-\frac{2GM}{r}\right)dt^2+\left(1+\frac{2GM}{r}\right)dr^2+r^2d\theta^2+r^2\sin^2\theta\,d\varphi^2-\frac{4GJ}{r}\sin^2\theta\,dtd\varphi, \tag{7.1}$$

where $J = Ma$ is the angular momentum of the star. In this background space-time a static and axially symmetric Maxwell field with a gauge-fixed vector-potential of the form:

$$A(r,\theta) = A_t(r,\theta)dt + A_\varphi(r,\theta)d\varphi,$$

satisfies the curved-space Maxwell equations

$$\begin{aligned}
&\left[\partial_r^2+\frac{2}{r}\partial_r+\frac{1}{r^2\sin\theta}\left(1+\frac{2GM}{r}\right)\partial_\theta\sin\theta\,\partial_\theta\right]A_t \\
&\qquad=-\frac{2GJ}{r^3}\left[\partial_r^2-\frac{1}{r}\,\partial_r+\frac{1}{r^2\sin\theta}\partial_\theta\sin\theta\partial_\theta\right]A_\varphi, \\
&\partial_r\left(\frac{1}{\sin\theta}\left(1-\frac{2GM}{r}\right)\partial_r A_\varphi\right)+\partial_\theta\left(\frac{1}{r^2\sin\theta}\partial_\theta A_\varphi\right) \\
&\qquad=\frac{2GJ\sin\theta}{r}\left[\partial_r^2-\frac{1}{r}\partial_r+\frac{1}{r^2\sin\theta}\partial_\theta\sin\theta\partial_\theta\right]A_t.
\end{aligned} \tag{7.2}$$

Note that we cannot impose A_t to vanish, unless $J = 0$. However, if we expand the solutions in powers of G, retaining only the terms to first order in G:

$$A_t = a_t + Gb_t, \qquad A_\varphi = a_\varphi + Gb_\varphi, \tag{7.3}$$

JCAP03(2025)065

and require the solutions to reduce to the corresponding Schwarzschild solution in the limit $J \to 0$, it follows that $a_t = 0$. As a result to this order the second equation (7.2) reduces to the same equation for A_φ as in the Schwarzschild case, except that here we should only retain the terms up to order G:

$$A_\varphi = \sum_{l=1}^{\infty} \frac{d_l}{r^l} \left(1 + \frac{l(l+2)}{l+1} \frac{GM}{r}\right) \Phi_l(\cos\theta). \tag{7.4}$$

Inserting this expression into the right-hand side of the first equation, to the first order in G only a_φ contributes:

$$\left(\partial_r^2 + \frac{2}{r}\,\partial_r + \frac{1}{r^2 \sin\theta} \partial_\theta \sin\theta\, \partial_\theta\right) b_t = -\frac{2J}{r^3} \left(\partial_r^2 - \frac{1}{r}\,\partial_r + \frac{1}{r^2 \sin\theta}\,\partial_\theta \sin\theta\, \partial_\theta\right) a_\varphi. \tag{7.5}$$

The solution of this equation reads

$$A_t = G b_t = -GJ \sum_{l=1}^{\infty} \frac{l d_l}{r^{l+3}}\, \cos\theta\, P_l(\cos\theta). \tag{7.6}$$

The coefficients d_l determine the relative strengths of the multipole components. From these expressions we now deduce the components of the electromagnetic field strength tensor; the non-vanishing magnetic components are

$$\begin{aligned} F_{r\varphi} &= -\sum_{l=1}^{\infty} \frac{l d_l}{r^{l+1}} \left(1 + (l+2)\frac{GM}{r}\right) \Phi_l(\cos\theta), \\ F_{\theta\varphi} &= \sum_{l\geq 1} \frac{l(l+1) d_l}{r^l} \left(1 + \frac{l(l+2)}{(l+1)}\,\frac{GM}{r}\right) \sin\theta\, P_l(\cos\theta), \end{aligned} \tag{7.7}$$

with corresponding non-vanishing electric components at order G:

$$\begin{aligned} F_{rt} &= GJ \sum_{l=1}^{\infty} \frac{l(l+3) d_l}{r^{l+4}}\, \cos\theta\, P_l(\cos\theta), \\ F_{\theta t} &= GJ \sum_{l=1}^{\infty} \frac{l d_l}{r^{l+3}}\, \sin\theta \left(P_l(\cos\theta) + \cos\theta P_l'(\cos\theta)\right). \end{aligned} \tag{7.8}$$

As the dependence on J indicates, the appearance of these electric components is clearly a result of the rotation of the gravitational field in the presence of static magnetic field components. Following the analysis in appendix B, the θ-component of the magnetic dipole field takes the standard form

$$B_\theta = \frac{\mu}{r^2}\, \sin\theta \left(1 + \mathcal{O}[G]\right),$$

after identifying $d_1 = \mu$. Of course, to first order in G higher-l multipoles are to be taken into account only as long as $d_{l+1} \gg \mu (GM)^l$.

JCAP03(2025)065

8 Equatorial orbits in slowly rotating background

As the metric (7.1) is axially symmetric and stationary, the energy and z-component of angular momentum of test particles are again constants of motion:

$$p_t = -m\varepsilon, \qquad p_\varphi = m\ell, \tag{8.1}$$

with

$$\begin{aligned} \varepsilon &= \left(1 - \frac{2GM}{r}\right) u^t + \frac{2GJ}{r} \sin^2\theta\, u^\varphi - \frac{q}{m} A_t, \\ \ell &= r^2 \sin^2\theta\, u^\varphi - \frac{2GJ}{r} \sin^2\theta\, u^t + \frac{q}{m} A_\varphi. \end{aligned} \tag{8.2}$$

By inverting these equations we get the proper velocity components involved:

$$\begin{aligned} u^t &= \left(1 + \frac{2GM}{r}\right)\varepsilon - \frac{2GJ\ell}{r^3} + \frac{q}{m}\left(A_t + \frac{2GJ}{r^3} A_\varphi\right), \\ u^\varphi &= \frac{1}{r^2 \sin^2\theta}\left(\ell - \frac{q}{m} A_\varphi\right) + \frac{2GJ}{r^3}\varepsilon, \end{aligned} \tag{8.3}$$

all expressions modulo terms $\mathcal{O}[G^2]$, keeping in mind that according to eq. (7.6) $A_t \sim \mathcal{O}[G]$.

Next observe, that the electric fields (7.8) vanish in the equatorial plane for odd multipoles; in fact for $l = 2n+1$ only the magnetic field component $F_{r\varphi}$ remains in the plane $\theta = \pi/2$. Therefore in the presence of dipole and other odd-multipole fields there exist solutions of the equations of motion (3.1) in the equatorial plane with $\sin\theta = 1$ and $u^\theta = 0$. On such orbits $A_t = 0$ and the hamiltonian constraint implies

$$u^{r\,2} = \varepsilon^2 - \left(1 - \frac{2GM}{r}\right)\left[1 + \frac{1}{r^2}\left(\ell - \frac{q}{m} A_\varphi\right)^2\right] - \frac{4GJ\varepsilon}{r^3}\left(\ell - \frac{q}{m} A_\varphi\right) + \mathcal{O}[G^2]. \tag{8.4}$$

For circular orbits with $r = R$ a constant, $u^\varphi = \omega_R$ a constant, $u^r = 0$ and $\dot{u}^r = 0$ it then follows that

$$\begin{aligned} \varepsilon^2 &= \left(1 - \frac{2GM}{R}\right)\left(1 + R^2\omega_R^2\right), \\ \left(1 - \frac{3GM}{R}\right)\omega_R^2 - \left[\frac{qB_\theta}{mR} - \frac{2GJ\varepsilon}{R^3}\right]\omega_R &= \frac{GM}{R^3}. \end{aligned} \tag{8.5}$$

For non-relativistic orbital velocities the last equation can be simplified (at order G) to give

$$\frac{2GJ\varepsilon}{R^3} \simeq \frac{2GJ}{R^3} + \frac{GJ\omega_R^2}{R}. \tag{8.6}$$

In this limit, and always up to terms of order $\mathcal{O}[G^2]$:

$$\left(1 - \frac{3GM}{R}\right)\omega_R^2 - \left(\frac{qB_\theta}{mR} - \frac{2GJ}{R^3}\right)\omega_R + \frac{GJ\omega_R^3}{R} = \frac{GM}{R^3}. \tag{8.7}$$

To check the stability of these orbits, we have again evaluated the world-line deviation equation (5.1) for the deviations n^θ out of the equatorial plane; using the results of appendix F we get

$$\ddot{n}^\theta = -\left[\omega_R^2 - \frac{2GJ\varepsilon}{R^3}\,\omega_R - \frac{q}{mR^2}\left(\partial_\theta F_{\theta\varphi}\omega_R + \partial_\theta F_{\theta t}\varepsilon\right)\right] n^\theta. \tag{8.8}$$

JCAP03(2025)065

In particular, for dipole fields:

$$\ddot{n}^\theta = -\left[\omega_R^2 - \frac{2GJ\varepsilon}{R^3}\,\omega_R + \frac{2q\mu\omega_R}{mR^3}\left(1+\frac{3GM}{2R}\right) - \frac{2q\mu GJ\varepsilon}{mR^6}\right] n^\theta. \tag{8.9}$$

This guarantees stability when

$$\frac{2GJ\varepsilon}{R^3} < \omega_R, \tag{8.10}$$

which is implicit in our approximation of a weakly rotating background geometry.

9 Discussion and summary

The starting point of this paper is the development of a multipole expansion for magnetic fields in a background Schwarzschild space-time and its generalization to slowly rotating stationary curved space-times. These results are valid in the case the back reaction of the magnetic field on the space-time geometry can be neglected. This is correct when the space-time curvature is large compared to the energy density in the magnetic field. Now the leading term in the dipole magnetic field gives the energy density in the equatorial plane as

$$\frac{\varepsilon_0}{2}\,\mathbf{B}^2 \simeq \frac{\varepsilon_0\mu^2}{4r^6}, \tag{9.1}$$

modulo higher-order corrections in G falling off faster. Higher multipoles also fall of faster than the dipole field. In contrast the curvature of Schwarzschild space-time satisfies

$$\sqrt{R_{\mu\nu\kappa\lambda}R^{\mu\nu\kappa\lambda}} = \frac{4\sqrt{3}GM}{r^3}. \tag{9.2}$$

Therefore the condition

$$8\pi G T_0{}^0 \ll \sqrt{R_{\mu\nu\kappa\lambda}R^{\mu\nu\kappa\lambda}}, \tag{9.3}$$

is satisfied everywhere if it is satisfied in the near-horizon region. Reinstating the speed of light, at the horizon the condition becomes

$$\frac{G\varepsilon_0\mathbf{B}^2}{c^2} \ll \left(\frac{c^2}{2GM}\right)^2. \tag{9.4}$$

For example, for neutron stars in the range of one to three solar masses this is satisfied for magnetic fields of 10^{15} T or less at the surface, which is about the observed upper limit.

Once the fields are known one can establish if stable circular orbits in the equatorial plane for charged particles are possible. This requires the radial magnetic field component to vanish in this plane, a condition always satisfied by odd-l multipole fields, like dipole and octopole fields. In the presence of even-l multipole fields such orbits can only exist for special radii where the odd multipole fields happen to cancel each other. Orbits within the stable photon orbit $3GM$ are possible in principle, provided the magnetic field strength exceeds the limit (4.6) and satisfies the stability conditions displayed in figure 4.

JCAP03(2025)065

In addition to circular orbits, for the case of Schwarzschild space-time we have also found approximate non-circular orbits by the method of relativistic epicycles (world-line deviations). In general the periods of the epicycles differ from the parent orbital period, which leads to displacement of the periastron of the charged particles. Moreover, in the presence of combinations of odd multipole fields the sign of the magnetic field can vary as a function of radial distance r, causing the direction of the rotation to change.

We have derived conditions for existence and stability of circular orbits in the equatorial plane, in particular in non-rotating Schwarzschild space-time. We found that the radius of innermost circular orbit and the innermost stable circular orbit can shift, for appropriately high values of the magnetic interaction, towards the black hole horizon. For the special case of a dipole magnetic field in a Schwarzschild spacetime, we found the existence of a 'forbidden region' in between the horizon and the photosphere where circular orbits are not allowed to exist, and two regions of stability where the circular orbits are allowed and stable in planar and transverse directions in a specific range of magnetic field strengths. In principle, these regions are most likely to host charged particles in circular orbits, resulting in distinct gravitational wave and electromagnetic frequencies. We have not considered their dynamical stability, due to the emission of gravitational or electromagnetic radiation. We expect these regions to have measurable consequences for the detection of magnetic fields around black holes and determining their strengths. This remains to be addressed in future research.

We have not constructed orbits in the transverse direction, out of the equatorial plane. In general such orbits will have a helical structure, as the Lorentz force will causs charged particles to circle around magnetic field lines. We have considered the effect of slow rotation of the background gravitational field, by considering the first-order in G approximation of the Kerr geometry. An interesting result is, that in that case also electric fields arise, both in the radial and the polar direction. However, again for odd-l multipoles these electric field components vanish in the equatorial plane, still allowing for stable circular orbits.

Topics discussed in the literature but not addressed in this paper include non-vacuum modifications of the Schwarzschild and Kerr metrics, discussed in [23], and euclidean extensions of the background geometry [24].

Finally we have not considered here the origin of the magnetic fields. As is well-known white dwarfs and neutron stars can have their own intrinsic magnetic fields. For black holes the source of magnetic fields, as observed by the Event-Horizon Telescope, must be currents of charged particles such as accretion disks circulating close to the black hole itself. This presents an intricate problem of magnetohydrodynamics; for rotating compact bodies there is an abundant literature on an effective description of such processes using the Blandford-Znajek scenario [25]; for recent discussions, see refs. [26–28].

A Schwarzschild geometry

In this appendix we summarize our conventions for the connection and curvature components of Schwarzschild geometry. Taking $c = 1$ the line-element in standard Schwarzschild-Droste co-ordinates reads

$$ds^2 = -\left(1 - \frac{2GM}{r}\right) dt^2 + \frac{dr^2}{1 - \frac{2GM}{r}} + r^2 d\theta^2 + r^2 \sin^2\theta \, d\varphi^2. \tag{A.1}$$

JCAP03(2025)065

The non-vanishing components of the corresponding Riemann-Christoffel connection are

$$\begin{aligned}
&\Gamma_{tt}{}^{r} = \frac{GM}{r^2}\left(1-\frac{2GM}{r}\right), && \Gamma_{rt}{}^{t} = \Gamma_{tr}{}^{t} = \frac{GM}{r^2\left(1-\frac{2GM}{r}\right)},\\
&\Gamma_{rr}{}^{r} = -\frac{GM}{r^2}\frac{1}{1-\frac{2GM}{r}}, && \\
&\Gamma_{\theta\theta}{}^{r} = -r\left(1-\frac{2GM}{r}\right), && \Gamma_{r\theta}{}^{\theta} = \Gamma_{\theta r}{}^{\theta} = \frac{1}{r},\\
&\Gamma_{\varphi\varphi}{}^{r} = -r\sin^2\theta\left(1-\frac{2GM}{r}\right), && \Gamma_{r\varphi}{}^{\varphi} = \Gamma_{\varphi r}{}^{\varphi} = \frac{1}{r},\\
&\Gamma_{\varphi\varphi}{}^{\theta} = -\sin\theta\cos\theta, && \Gamma_{\theta\varphi}{}^{\varphi} = \Gamma_{\varphi\theta}{}^{\varphi} = \operatorname{cotg}\theta,
\end{aligned} \tag{A.2}$$

whilst the non-vanishing components of the Riemann curvature tensor are given by

$$\begin{aligned}
&R_{trt}{}^{r} = \frac{2GM}{r^3}\left(1-\frac{2GM}{r}\right), && R_{rtr}{}^{t} = -\frac{2GM}{r^3\left(1-\frac{2GM}{r}\right)},\\
&R_{t\theta t}{}^{\theta} = -\frac{GM}{r^3}\left(1-\frac{2GM}{r}\right), && R_{\theta t\theta}{}^{t} = \frac{GM}{r},\\
&R_{t\varphi t}{}^{\varphi} = -\frac{GM}{r^3}\left(1-\frac{2GM}{r}\right), && R_{\varphi t\varphi}{}^{t} = \frac{GM}{r}\sin^2\theta,
\end{aligned} \tag{A.3}$$

and

$$\begin{aligned}
&R_{r\theta r}{}^{\theta} = \frac{GM}{r^3\left(1-\frac{2GM}{r}\right)}, && R_{\theta r\theta}{}^{r} = \frac{GM}{r},\\
&R_{r\varphi r}{}^{\varphi} = \frac{GM}{r^3\left(1-\frac{2GM}{r}\right)}, && R_{\varphi r\varphi}{}^{r} = \frac{GM}{r}\sin^2\theta,\\
&R_{\theta\varphi\theta}{}^{\varphi} = -\frac{2GM}{r}, && R_{\varphi\theta\varphi}{}^{\theta} = -\frac{2GM}{r}\sin^2\theta.
\end{aligned} \tag{A.4}$$

B Magnetic fields in Schwarzschild space-time

We describe electromagnetic fields in Schwarzschild space-time in the frame of a static distant observer associated with the Schwarzschild-Droste co-ordinate system (A.1). In the absence of electric components, any static magnetic fields can be derived in the radial gauge $A_r = 0$ from a vector potential 1-form

$$A = A_\theta\, d\theta + A_\varphi\, d\varphi.$$

Imposing axial symmetry then implies that the components are functions of (r, θ) only. As a result the magnetic field strength $F_{ij} = \partial_i A_j - \partial_j A_i$ has components

$$F_{r\theta} = \partial_r A_\theta, \qquad F_{r\varphi} = \partial_r A_\varphi, \qquad F_{\theta\varphi} = \partial_\theta A_\varphi. \tag{B.1}$$

The Maxwell equations for the magnetic field strength components (B.1) in the presence of a current density j^i then reduce to

$$\partial_j\left(\sqrt{-g}F^{ji}\right) = \partial_j\left(\sqrt{-g}\, g^{jk}g^{il}F_{kl}\right) = \sqrt{-g}\, j^i. \tag{B.2}$$

JCAP03(2025)065

Written out separately for $i = (r, \theta, \varphi)$:

$$\begin{aligned} \partial_\theta \left(\sqrt{-g}\, g^{\theta\theta} g^{rr} F_{r\theta} \right) &= \sqrt{-g}\, j^r, \\ \partial_r \left(\sqrt{-g}\, g^{rr} g^{\theta\theta} F_{r\theta} \right) &= \sqrt{-g}\, j^\theta, \\ \partial_r \left(\sqrt{-g}\, g^{rr} g^{\varphi\varphi} F_{r\varphi} \right) + \partial_\theta \left(\sqrt{-g}\, g^{\theta\theta} g^{\varphi\varphi} F_{\theta\varphi} \right) &= \sqrt{-g}\, j^\varphi. \end{aligned} \tag{B.3}$$

In the absence of radial and polar currrents: $j^r = j^\theta = 0$, the first two equations imply that

$$F_{r\theta} = \frac{\kappa}{\sqrt{-g}}\, g_{rr} g_{\theta\theta}, \tag{B.4}$$

with κ a constant; in Schwarzschild space-time this becomes

$$F_{r\theta} = \frac{\kappa}{\sin\theta} \frac{1}{1 - \frac{2GM}{r}}. \tag{B.5}$$

This solution is singular everywhere on the z-axis as well as on the horizon. Therefore we discard it by setting $A_\theta = 0$.

Finally, evaluation of the third equation (B.3) yields the result [4]

$$r^2 \partial_r \left[\left(1 - \frac{2GM}{r} \right) \partial_r A_\varphi \right] + \sin\theta \partial_\theta \left[\frac{1}{\sin\theta} \partial_\theta A_\varphi \right] = -r^4 \sin^2\theta\, j^\varphi,$$

which is defines the starting point eq. (2.1) for the discussion in section 2.

The relation between the magnetic field strength components F_{ij} and the dual axial vector field B_i is defined in terms of the antisymmetric permutation tensor

$$E_{\mu\nu\rho\sigma} = \sqrt{-g}\, \varepsilon_{\mu\nu\rho\sigma} = r^2 \sin\theta\, \varepsilon_{\mu\nu\rho\sigma}, \tag{B.6}$$

with $\varepsilon_{\mu\nu\rho\sigma} = +1$ for even permutations of $(\mu\nu\rho\sigma) = (tr\theta\varphi)$, $\varepsilon_{\mu\nu\rho\sigma} = -1$ for odd permutations of $(\mu\nu\rho\sigma) = (tr\theta\varphi)$, and $\varepsilon_{\mu\nu\rho\sigma} = 0$ in all other cases. Its inverse is

$$E^{\mu\nu\rho\sigma} = \frac{1}{\sqrt{-g}}\, \varepsilon^{\mu\nu\rho\sigma} = \frac{1}{r^2 \sin\theta}\, \varepsilon^{\mu\nu\rho\sigma}, \tag{B.7}$$

with $\varepsilon^{\mu\nu\rho\sigma} = -1$ for even permutations of $(\mu\nu\rho\sigma) = (tr\theta\varphi)$ and $\varepsilon_{\mu\nu\rho\sigma} = +1$ for odd permutations of $(\mu\nu\rho\sigma) = (tr\theta\varphi)$. With these definitions the dual electromagnetic field strength is

$$\tilde{F}^{\mu\nu} = \frac{1}{2}\, E^{\mu\nu\rho\sigma} F_{\rho\sigma}, \tag{B.8}$$

and the B-field components are defined by

$$B_i = \tilde{F}_{0i} = g_{00} g_{ij} \tilde{F}^{0j} = -\frac{1}{2\sqrt{-g}}\, g_{00} g_{ij} \varepsilon^{jkl} F_{kl}. \tag{B.9}$$

Therefore in Schwarzschild space-time

$$B_r = \frac{1}{r^2 \sin\theta}\, F_{\theta\varphi}, \quad B_\theta = -\frac{1}{\sin\theta} \left(1 - \frac{2GM}{r} \right) F_{r\varphi}, \quad B_\varphi = \left(1 - \frac{2GM}{r} \right) F_{r\theta}. \tag{B.10}$$

The vanishing of the field-strength component $F_{r\theta}$ is seen to be equivalent to $B_\varphi = 0$.

JCAP03(2025)065

C Angular dependence of magnetic fields

The angular dependence of the magnetic fields discussed in this paper is expressed in terms of Legendre polynomials $P_l(\cos\theta)$ and the related functions $\Phi_l(\cos\theta)$ derived in section 2. Here we give explicit expressions for the cases $l = 1, 2, 3, 4$, or dipole, quadrupole, octopole and hexadecapole fields. Writing $x = \cos\theta$:

$$\begin{aligned} &P_0(x) = 1, && P_1(x) = x, && P_2(x) = \frac{1}{2}\left(3x^2 - 1\right), \\ &P_3(x) = \frac{1}{2}\left(5x^3 - 3x\right), && P_4(x) = \frac{1}{8}\left(35x^4 - 30x^2 + 3\right), \end{aligned} \tag{C.1}$$

and

$$\begin{aligned} &\Phi_1(x) = -\left(x^2 - 1\right), && \Phi_2(x) = -3\left(x^3 - x\right), \\ &\Phi_3(x) = -\frac{3}{2}\left(5x^4 - 6x^2 + 1\right), && \Phi_4(x) = -\frac{5}{2}\left(7x^5 - 10x^3 + 3x\right). \end{aligned} \tag{C.2}$$

D Radial dependence of magnetic fields

In this appendix we provide details of the solutions for the radial dependence of the magnetic vector potential A_φ. We first consider the series solution in inverse powers of r. Switching to the new variable $\eta = 2GM/r$ the first equation (2.3) takes the form

$$\frac{d}{d\eta}\left[\eta^2\left(1-\eta\right)\frac{df_l}{d\eta}\right] = \left(\eta^2 - \eta^3\right)\frac{d^2 f_l}{d\eta^2} + \left(2\eta - 3\eta^2\right)\frac{df_l}{d\eta} = l(l+1)\, f_l. \tag{D.1}$$

With the Ansatz

$$f_l(\eta) = \sum_{n=0}^{\infty} c_n^{(l)} \eta^n, \tag{D.2}$$

this becomes

$$\begin{aligned} &l(l+1)\, c_0^{(l)} + \left[l(l+1) - 2\right] c_1^{(l)}\eta + \left[\left(l(l+1) - 6\right) c_2^{(l)} + 3c_1^{(l)}\right]\eta^2 \\ &\quad + \sum_{n=3}^{\infty}\left[\left(l(l+1) - n(n+1)\right) c_n^{(l)} + (n-1)(n+1)\, c_{n-1}^{(l)}\right]\eta^n = 0. \end{aligned} \tag{D.3}$$

Since this is to hold for any η, it follows that $c_0^{(l)} = 0$ and for any $k \geq 1$:

$$c_{l-k}^{(l)} = 0, \quad c_{l+k}^{(l)} = \frac{(l+k)^2 - 1}{k(2l+k+1)}\, c_{l+k-1}^{(l)}. \tag{D.4}$$

The upshot is, that $c_l^{(l)}$ is a free parameter, and higher coefficients are related to this parameter by

$$c_{l+k}^{(l)} = \frac{1}{k!}\prod_{m=1}^{k}\left(\frac{(l+m)^2 - 1}{2l+m+1}\right) c_l^{(l)}. \tag{D.5}$$

JCAP03(2025)065

The first few series then start out as

$$
\begin{aligned}
f_1(\eta) &= c_1^{(1)}\eta\left(1+\frac{3}{4}\,\eta+\frac{3}{5}\,\eta^2+\frac{1}{2}\,\eta^3+\dots\right),\\
f_2(\eta) &= c_2^{(2)}\eta^2\left(1+\frac{4}{3}\,\eta+\frac{10}{7}\,\eta^2+\frac{10}{7}\,\eta^3+\dots\right),\\
f_3(\eta) &= c_3^{(3)}\eta^3\left(1+\frac{15}{8}\,\eta+\frac{5}{2}\,\eta^2+\frac{35}{12}\,\eta^3+\dots\right).
\end{aligned}
\tag{D.6}
$$

Up to the normalization factor these series can actually be summed and written in closed form:

$$
\begin{aligned}
f_1(\eta) &= -\frac{3}{\eta^2}\left[\ln(1-\eta)+\eta+\frac{\eta^2}{2}\right],\\
f_2(\eta) &= -\frac{20}{\eta^3}\left[(4-3\eta)\ln(1-\eta)+4\eta-\eta^2-\frac{\eta^3}{6}\right],\\
f_3(\eta) &= -\frac{105}{\eta^4}\left[\left(15-20\eta+6\eta^2\right)\ln(1-\eta)+15\eta-\frac{25}{2}\,\eta^2+\eta^3+\frac{\eta^4}{12}\right].
\end{aligned}
\tag{D.7}
$$

These solutions all have a logarithmic divergence on the horizon $\eta = 1$. They are equivalent to the closed-form expressions (2.15), (2.16) derived in [4, 8]. As mentioned in section 2, in addition to these solutions valid for $r > 2GM$ there also exist polynomial solutions of the radial equation in the domain $0 \le r < \infty$. We denoted these solutions by $g_l(z)$, where by definition $z = 1/\eta = r/2GM$; equation (2.3) then becomes:

$$
z^2\frac{d}{dz}\left[\left(1-\frac{1}{z}\right)\frac{dg_l}{dz}\right] = z(z-1)\frac{d^2g_l}{dz^2}+\frac{dg_l}{dz} = l\,(l+1)\,g_l. \tag{D.8}
$$

Looking for solutions

$$
g_l(z) = \sum_{n=0}^{\infty} a_n^{(l)} z^n, \tag{D.9}
$$

by substitution in (D.8) this equation becomes

$$
\begin{aligned}
0 = {} & l(l+1)\,a_0^{(l)} - a_1^{(l)} + l(l+1)\,a_1^{(l)} z\\
& + \sum_{n\ge 2}\left[(n-1)(n+1)a_{n+1}^{(l)} + \left(l(l+1)-n(n-1)\right)a_n^{(l)}\right] z^n.
\end{aligned}
\tag{D.10}
$$

It follows that $a_0^{(l)} = a_1^{(l)} = 0$ and for $n \ge 2$

$$
a_{n+1}^{(l)} = \frac{n(n-1)-l(l+1)}{(n-1)(n+1)}\,a_n^{(l)}. \tag{D.11}
$$

Then for all $k \ge 2$ also $a_{l+k}^{(l)} = 0$, and the solutions become polynomials of order $l+1$:

$$
g_l(z) = \sum_{n=2}^{l+1} a_n^{(l)} z^n, \tag{D.12}
$$

JCAP03(2025)065

with $a_2^{(l)}$ a free parameter and all coefficients $a_{2+k}^{(l)}$ defined by

$$a_{2+k}^{(l)} = \prod_{m=1}^{k} \left(\frac{m(m+1) - l(l+1)}{m(m+2)} \right) a_2^{(l)}, \quad k = 1, \ldots, l-1. \tag{D.13}$$

The first few polynomials are

$$\begin{aligned} g_1(z) &= a_2^{(1)} z^2, & g_2(z) &= a_2^{(2)} z^2 \left(1 - \frac{4}{3} z\right), \\ g_3(z) &= a_2^{(3)} z^2 \left(1 - \frac{10}{3} z + \frac{5}{2} z^2\right), & g_4(z) &= a_2^{(4)} z^2 \left(1 - 6z + \frac{21}{2} z^2 - \frac{28}{5} z^3\right). \end{aligned} \tag{D.14}$$

For $1 < r < \infty$ both the asymptotic solutions or the polynomial solutions exist. In fact, as pointed out in [4] there is a direct relation between these two sets of solutions:

$$f_l(1/z) = \beta_l \, g_l(z) \int_z^\infty \frac{d\zeta}{\left(1 - \frac{1}{\zeta}\right) g_l^2(\zeta)}. \tag{D.15}$$

The solutions (D.7) correspond to specific choices of the normalization factor β_l, specifically $\beta_1 = 3$, $\beta_2 = 20/3$, $\beta_3 = 35/2$. An equivalent integral expression for the asymptotic solutions $f_l(r) = r^2 \mathcal{Q}_{l-2}^{(0,2)} \left(\frac{r}{GM} - 1\right)$ is given in [8].

E Stability analysis for circular dipole orbits

In section 6 we discussed the stability of circular orbits in dipole magnetic fields. This appendix presents the details of the analysis on which the results about stability are based. The input of this analysis is first the condition of existence of circular orbits, and second the periodicity of the fluctuations about these orbits, expressed by the reality of the frequencies of the transverse and planar deviations. In terms of the dimensionless variables (6.1) these conditions are summarized by eqs. (6.6), (6.10) and (6.12). The complication of analyzing these conditions is, that they need to be considered separately in different domains of variables: $2 < x < 3$, $3 < x < 6$ and $x > 6$; and that they have to be discussed for two choices of sign in the relation between the angular velocity Ω and equatorial magnetic field y. We first discuss the choice of positive sign:

$$2(x-3)\Omega = y \left(1 + \sqrt{1 + \frac{4(x-3)}{x^2 y^2}}\right). \tag{E.1}$$

This relation imposes the inequality (6.6), which is trivially satisfied for $x \geq 3$; but for $2 < x < 3$ it requires a non-zero magnetic field:

$$y^2 > \frac{4(3-x)}{x^2}. \tag{E.2}$$

Next, the inequality (6.10) for transverse stability becomes

$$\sqrt{1 + \frac{4(x-3)}{x^2 y^2}} > -\left(1 + \frac{4(x-3)k(x)}{x h(x)}\right). \tag{E.3}$$

JCAP03(2025)065

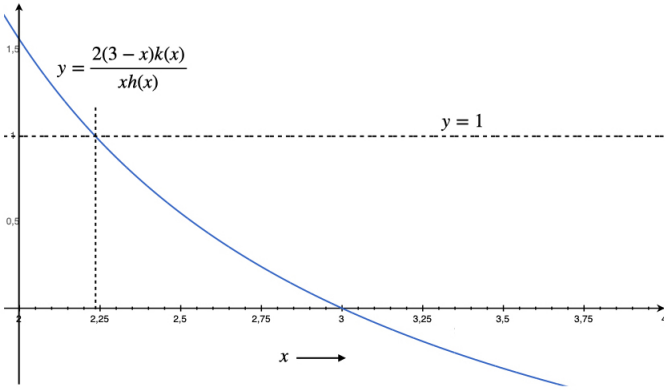

Figure 5. Range of x for which $2 < x < 3$ and $2(3-x)k(x)/xh(x) < 1$.

Again, it is satisfied for all y in the range (E.2) if the r.h.s. is negative, which happens if

$$xh(x) \geq 4(3-x)k(x). \tag{E.4}$$

This is true automatically for $x \geq 3$; if $xh(x) < 4(3-x)k(x)$ the case $2 < x < 3$ has to be considered separately. Terms on both sides of the inequality can then be squared and rearranged to give

$$y^2 > \frac{4(3-x)}{x^2} \frac{1}{1-\left(\frac{4(3-x)k(x)}{xh(x)}-1\right)^2}. \tag{E.5}$$

Non-trivial solutions of this inequality implying transverse stability (E.3) exist only in the domain

$$0 < \frac{2(3-x)k(x)}{xh(x)} < 1, \tag{E.6}$$

or approximately $2.23 < x < 3$; see figure 5.

In summary, either $x \geq 3$ for all values of y^2, or $2.23 < x < 3$ and y^2 in the range

$$y^2 > \frac{4(3-x)}{x^2} \frac{1}{1-\left(1-\frac{4(3-x)k(x)}{xh(x)}\right)^2} > \frac{4(3-x)}{x^2}. \tag{E.7}$$

Finally it remains to consider the condition for planar stabilty, expressed by the inequality (6.12), which can be recast in the form

$$\frac{(x-2)(x-3)(x-6)}{x^2y^2} + (x-3)^2 - F(x)\left(1+\sqrt{1+\frac{4(x-3)}{x^2y^2}}\right) \geq 0, \tag{E.8}$$

where

$$F(x) \equiv \frac{1}{2}\left(x^2 - 4x + 6 + 2(x-2)(x-3)\frac{k(x)}{h(x)}\right). \tag{E.9}$$

Figure 6 shows that in the domain $x > 2$ this function is everywhere positive. For comparison we have also plotted the function $(x-3)^2/2$ to show that

$$2F(x) > (x-3)^2.$$

JCAP03(2025)065

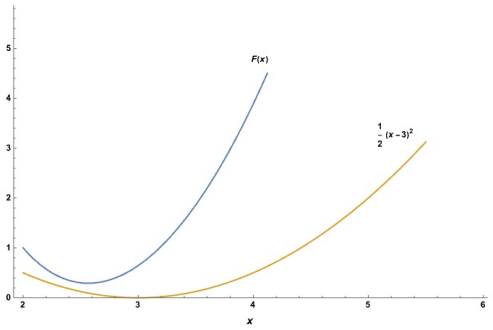

Figure 6. The function $F(x)$ defined in eq. (E.9).

This implies that the inequality (E.8) is never satisfied in the limit $y^2 \to \infty$; thus it imposes restrictions on the allowed values of the magnetic field as represented by y. Defining the coefficients

$$A = (x-2)^2(x-3)^2(x-6)^2,$$
$$B = x^2(x-3)\left[(x-2)(x-6)\left(F(x)-(x-3)^2\right)+2F^2(x)\right],$$
$$C = x^4(x-3)^2\left(F(x)-\frac{1}{2}(x-3)^2\right),$$

and considering the domain $x > 6$ where $(x-2)(x-3)(x-6) > 0$ and $(A, B, C) > 0$ everywhere, the condition of planar stability reduces to

$$\frac{A}{y^4} - \frac{2B}{y^2} - 2C \geq 0,$$

which is solved for

$$y^2 \leq \frac{A}{B+\sqrt{B^2+2AC}}. \tag{E.10}$$

For $3 < x < 6$ it follows that $(x-2)(x-3)(x-6) < 0$; in that domain

$$\frac{(x-2)(x-3)(x-6)}{x^2y^2} + (x-3)^2 - F(x)\left(1+\sqrt{1+\frac{4(x-3)}{x^2y^2}}\right) < 0;$$

thus the condition (E.8) for planar stability has no solutions. Finally, for $2 < x < 3$ the coefficient $A > 0$, but B can become negative; however, as $\sqrt{B^2+2AC} > |B|$ there are still non-trivial solutions for y in the domain defined by (E.10), provided (E.2) holds:

$$\frac{4(3-x)}{x^2} \leq y^2 \leq \frac{A}{B+\sqrt{B^2+2AC}}. \tag{E.11}$$

It remains to investigate the stability of circular orbits for which

$$2(x-3)\Omega = y\left(1-\sqrt{1+\frac{4(x-3)}{x^2y^2}}\right). \tag{E.12}$$

JCAP03(2025)065

Again we have to distinguish the domains $x > 3$ and $2 < x < 3$; in both cases $y/\Omega < 0$ and therefore the inequality (6.8) becomes non-trivial:

$$0 > \frac{y}{\Omega} = \frac{2(x-3)}{1-\sqrt{1+\frac{4(x-3)}{x^2y^2}}} > -\frac{xh(x)}{2k(x)}. \tag{E.13}$$

For $x > 3$ this imposes the explicit constraint

$$0 < y^2 < \frac{4(x-3)}{x^2}\frac{1}{\left(1+\frac{4(x-3)k(x)}{xh(x)}\right)^2-1}. \tag{E.14}$$

For $2 < x < 3$ we get

$$y^2 < \frac{4(3-x)}{x^2}\frac{1}{1-\left(\frac{4(3-x)k(x)}{xh(x)}-1\right)^2}, \tag{E.15}$$

with x in the range (E.6); see figure 5.

Finally, we have to impose the inequality (6.12), which in this case becomes

$$\frac{(x-2)(x-3)(x-6)}{x^2y^2} + (x-3)^2 + F(x)\left(\sqrt{1+\frac{4(x-3)}{x^2y^2}}-1\right) \geq 0. \tag{E.16}$$

For $x > 6$ it is always satisfied. Next, for $3 < x < 6$ it still holds in the limit $y^2 \to \infty$, but there is a lower threshold

$$y^2 \geq \frac{A}{B+\sqrt{B^2+2AC}}. \tag{E.17}$$

In the remaining domain $2 < x < 3$ the situation is similar, but there is the additional condition (E.2); therefore the condition for stability of circular orbits in the plane becomes

$$y^2 \geq \max\left(\frac{A}{B+\sqrt{B^2+2AC}}, \frac{4(3-x)}{x^2}\right). \tag{E.18}$$

F Weak field limit of Kerr geometry

The weak-field approximation of Kerr geometry, deviating from Minkowski space-time only by terms linear in G, is described by the line element (7.1). Based on this, the expressions for the components of the connection to first order in G read

$$\begin{aligned}
&\Gamma_{rr}{}^{r} = -\frac{GM}{r^2}, && \Gamma_{\theta\theta}{}^{r} = -r\left(1-\frac{2GM}{r}\right), && \Gamma_{r\theta}{}^{\theta} = \frac{1}{r},\\
&\Gamma_{\varphi\varphi}{}^{r} = -r\sin^2\theta\left(1-\frac{2GM}{r}\right), && \Gamma_{r\varphi}{}^{\varphi} = \frac{1}{r}, &&\\
&\Gamma_{tt}{}^{r} = \frac{GM}{r^2}, && \Gamma_{rt}{}^{t} = \frac{GM}{r^2}, &&\\
&\Gamma_{\varphi\varphi}{}^{\theta} = -\sin\theta\cos\theta, && \Gamma_{\theta\varphi}{}^{\varphi} = \frac{\cos\theta}{\sin\theta}, &&\\
&\Gamma_{r\varphi}{}^{t} = -\frac{3GJ}{r^2}\sin^2\theta, && \Gamma_{rt}{}^{\varphi} = \frac{GJ}{r^4}, && \Gamma_{t\varphi}{}^{r} = -\frac{GJ}{r^2}\sin^2\theta,\\
&\Gamma_{\theta\varphi}{}^{t} = \frac{GJ}{r}\sin\theta\cos\theta, && \Gamma_{t\theta}{}^{\varphi} = -\frac{GJ}{r^3}\frac{\cos\theta}{\sin\theta}, && \Gamma_{t\varphi}{}^{\theta} = \frac{GJ}{r^3}\sin\theta\cos\theta.
\end{aligned} \tag{F.1}$$

JCAP03(2025)065

Non-zero θ-components of the Riemann tensor:

$$R_{t\theta t}{}^{\theta} = -\frac{GM}{r^3}, \qquad R_{r\theta r}{}^{\theta} = \frac{GM}{r^3},$$
$$R_{\varphi\theta\varphi}{}^{\theta} = -\frac{2GM}{r}\sin^2\theta, \qquad R_{t\theta\varphi}{}^{\theta} = \frac{2GJ}{r^3}\sin^2\theta, \tag{F.2}$$

References

[1] Event Horizon Telescope collaboration, *First M87 Event Horizon Telescope Results. VIII. Magnetic Field Structure near The Event Horizon*, *Astrophys. J. Lett.* **910** (2021) L13 [arXiv:2105.01173] [INSPIRE].

[2] A. Nathanail, P. Dhang and C.M. Fromm, *Magnetic field structure in the vicinity of a supermassive black hole in low-luminosity galaxies: the case of Sgr A**, *Mon. Not. Roy. Astron. Soc.* **513** (2022) 5204 [arXiv:2205.12287] [INSPIRE].

[3] R.M. Wald, *Black hole in a uniform magnetic field*, *Phys. Rev. D* **10** (1974) 1680 [INSPIRE].

[4] J.A. Petterson, *Magnetic field of a current loop around a Schwarzschild black hole*, *Phys. Rev. D* **10** (1974) 3166 [INSPIRE].

[5] J.A. Petterson, *Stationary axisymmetric electromagnetic fields around a rotating black hole*, *Phys. Rev. D* **12** (1975) 2218 [INSPIRE].

[6] B. Linet, *Dipole field solution of Maxwell's equations in the Schwarzschild metric*, *J. Phys. A* **8** (1975) 328 [INSPIRE].

[7] J. Bičák and L. Dvořák, *Stationary electromagnetic fields around black holes. I. General solutions and the fields of some special sources near a Schwarzschild black hole*, *Czech. J. Phys. B* **27** (1977) 127.

[8] P. Ghosh, *The Structure of black hole magnetospheres. 1. Schwarzschild black holes*, *Mon. Not. Roy. Astron. Soc.* **315** (2000) 89 [astro-ph/9907427] [INSPIRE].

[9] H. Li and J. Wang, *Expanded solutions of force-free electrodynamics on general Kerr black holes*, *Phys. Rev. D* **96** (2017) 023014 [arXiv:1705.08757] [INSPIRE].

[10] V. Karas, *Astrophysical black holes embedded in organized magnetic fields: Case of a nonvanishing electric charge*, in the proceedings of the *25th Relativistic Astrophysics Group Meeting (RAGtime 25)*, Opava, Czech Republic, 27 November–1 December 2023, S. Hledík and Z. Stuchlík eds., Silesian University, Opava, Czech Republic (2023), pp. 13–19 [arXiv:2301.00684] [INSPIRE].

[11] A.R. Prasanna, *General-relativistic analysis of charged-particle motion in electromagnetic fields surrounding black holes*, *Riv. Nuovo Cim.* **3** (1980) 1.

[12] G. Preti, *On charged particle orbits in dipole magnetic fields around Schwarzschild black holes*, *Class. Quant. Grav.* **21** (2004) 3433.

[13] V.P. Frolov and A.A. Shoom, *Motion of charged particles near weakly magnetized Schwarzschild black hole*, *Phys. Rev. D* **82** (2010) 084034 [arXiv:1008.2985] [INSPIRE].

[14] P. Bakala et al., *Non-geodesic orbital and epicyclic frequencies in vicinity of slowly rotating magnetized neutron stars*, in the proceedings of the *Feeding Compact Objects: Accretion on All Scales*, Beijing, China, 20–24 August 2012, C.M. Zhang, T. Belloni, M. Mendez and S.N. Zhang eds., Cambridge University Press, Cambridge, U.K. (2013) [*Proc. Int. Astron. Union* **8** (2013) 185] [arXiv:1212.6938] [INSPIRE].

JCAP03(2025)065

[15] R. Shiose, M. Kimura and T. Chiba, *Motion of Charged Particles around a Weakly Magnetized Rotating Black Hole*, *Phys. Rev. D* **90** (2014) 124016 [arXiv:1409.3310] [INSPIRE].

[16] J.P. Hackstein and E. Hackmann, *Influence of weak electromagnetic fields on charged particle ISCOs*, *Gen. Rel. Grav.* **52** (2020) 22 [arXiv:1911.07645] [INSPIRE].

[17] N.P. Baker and V.P. Frolov, *Charged particle motion near a magnetized black hole: A near-horizon approximation*, *Phys. Rev. D* **108** (2023) 024045 [arXiv:2305.12591] [INSPIRE].

[18] A. Balakin, J.W. van Holten and R. Kerner, *Motions and worldline deviations in Einstein-Maxwell theory*, *Class. Quant. Grav.* **17** (2000) 5009 [gr-qc/0009016] [INSPIRE].

[19] R. Colistete Jr., R. Kerner and J.W. van Holten, *Relativistic epicycles: Another approach to geodesic deviations*, *Class. Quant. Grav.* **18** (2001) 4725 [gr-qc/0102099] [INSPIRE].

[20] R. Colistete Jr., C. Leygnac and R. Kerner, *Higher order geodesic deviations applied to the Kerr metric*, *Class. Quant. Grav.* **19** (2002) 4573 [gr-qc/0205019] [INSPIRE].

[21] G. Koekoek and J.W. van Holten, *Epicycles and Poincaré Resonances in General Relativity*, *Phys. Rev. D* **83** (2011) 064041 [arXiv:1011.3973] [INSPIRE].

[22] J.-W. van Holten, *World-line perturbation theory*, in *Relativistic Geodesy*, *Fundamental Theories of Physics* **196**, D. Puetzfeld and C. Lämmerzahl eds., Springer, Cham, Switzerland (2019), pp. 393–418 [DOI:10.1007/978-3-030-11500-5_12] [arXiv:1611.08824] [INSPIRE].

[23] M. Azreg-Aïnou, *Vacuum and nonvacuum black holes in a uniform magnetic field*, *Eur. Phys. J. C* **76** (2016) 414 [arXiv:1603.07894] [INSPIRE].

[24] E. Battista and G. Esposito, *Geodesic motion in Euclidean Schwarzschild geometry*, *Eur. Phys. J. C* **82** (2022) 1088 [arXiv:2202.03763] [INSPIRE].

[25] R.D. Blandford and R.L. Znajek, *Electromagnetic extractions of energy from Kerr black holes*, *Mon. Not. Roy. Astron. Soc.* **179** (1977) 433 [INSPIRE].

[26] S. Kinoshita and T. Igata, *The essence of the Blandford-Znajek process*, *Prog. Theor. Exp. Phys.* **2018** (2018) 033E02 [arXiv:1710.09152] [INSPIRE].

[27] J. Armas et al., *Consistent Blandford-Znajek Expansion*, *JCAP* **04** (2020) 009 [arXiv:2002.01972] [INSPIRE].

[28] F. Camilloni et al., *Blandford-Znajek monopole expansion revisited: novel non-analytic contributions to the power emission*, *JCAP* **07** (2022) 032 [arXiv:2201.11068] [INSPIRE].

JCAP03(2025)065